THE JOURNAL OF PHYSICAL CHEMISTRY B

Article

pubs.acs.org/JPCB

Ab Initio Molecular Dynamics Simulation of Proton Hopping in a Model Polymer Membrane

Ram Devanathan,* Nagesh Idupulapati,† Marcel D. Baer, Christopher J. Mundy, and Michel Dupuis

Physical Sciences Division, MS K2-01, Pacific Northwest National Laboratory, Richland, Washington 99352, United States

Supporting Information

ABSTRACT: We report the results of ab initio molecular dynamics simulations of a model Nafion polymer membrane initially equilibrated using classical molecular dynamics simulations. We studied three hydration levels (λ) of 3, 9, and 15 H_2O/SO_3^- corresponding to dry, hydrated, and saturated fuel cell membrane, respectively. The barrier for proton transfer from the SO_3^-−H_3O^+ contact ion pair to a solvent-separated ion pair decreased from 2.3 kcal/mol for λ = 3 to 0.8 kcal/mol for λ = 15. The barrier for proton transfer between two water molecules was in the range from 0.7 to 0.8 kcal/mol for the λ values studied. The number of proton shuttling events between a pair of water molecules is an order of magnitude more than the number of proton hops across three distinct water molecules. The proton diffusion coefficient at λ = 15 is about 0.9×10^{-5} cm^2/s, which is in good agreement with experiment and our previous quantum hopping molecular dynamics simulations.

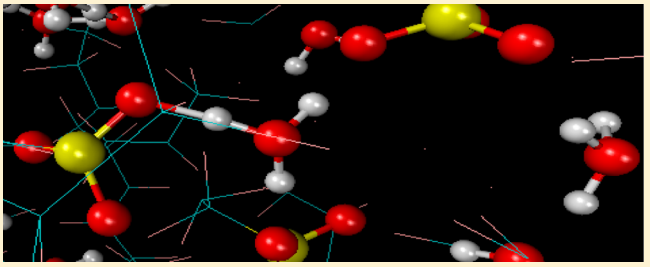

I. INTRODUCTION

Proton transport in complex chemical environments is of broad interest, because of its important role in biological systems and engineered devices, such as fuel cells.[1] At the fundamental level, elementary steps in the proton transfer process and the role of chemistry and confinement on proton transport are of longstanding scientific interest.[2] Understanding and controlling proton transport is essential to advance our knowledge of chemical and biological processes and to develop biomimetic devices for efficient energy conversion.[3] In this regard, polymer electrolyte membrane, also known as proton exchange membrane, (PEM) fuel cells have considerable potential for deployment in portable power, transportation, and off-grid power applications. These devices convert chemical energy of fuel, such as hydrogen, methane, or methanol, to electrical energy efficiently, quietly, and without pollution. The widespread adoption of this technology can improve energy security and reduce the adverse environmental impact of energy use, but progress has been hampered by high cost and poor fuel cell reliability under prolonged high temperature operation. Much of PEM fuel cell research has focused on the membrane-electrode assembly[4] at the center of the device, where a 0.1 mm thin polymer membrane serves as a barrier to small molecules while conducting protons. The pressing technological need is to develop durable and inexpensive membranes that can operate under minimally hydrated conditions above 120 °C so that the electrocatalysts can function efficiently without being poisoned by CO. Such an effort has to be underpinned by systematic studies of the effect of membrane hydration on proton transport using molecular modeling validated by experiment.[5]

The ideal membrane for studying proton transport under different hydration levels (λ), usually expressed in units of H_2O molecules per SO_3^- group, is Nafion developed by DuPont Inc. This random polymer features a hydrophobic poly tetrafluoroethylene backbone with a side chain terminated by a perfluorosulfonic acid pendant. The backbone length, side chain length and chemistry can be varied to modify the transport properties. Nafion has been extensively studied for nearly half a century and there is extensive experimental[6] and modeling data[5,7,8] available for validation. It performs well in PEM fuel cells at temperatures below 85 °C, although there are concerns about cost, electro-osmotic drag of water molecules with protons, and fuel (methanol) passing through the membrane (crossover). Nafion still serves as the benchmark against which other membranes are compared and rated. However, despite extensive study, the molecular-level details of membrane morphology, proton hopping, and small molecule transport are poorly understood, because the dynamical processes at subnanometer and subnanosecond scales are not readily accessible to experiments. For instance, there exist several different models of the morphology of hydrated Nafion without conclusive evidence in favor of a particular representation.[6,9,10]

Computer simulation starting from the molecular level with ab initio calculations and extending beyond the nanometer scale with mesoscale methods and continuum models can complement experimental understanding by filling knowledge

Received: October 15, 2013
Revised: December 6, 2013
Published: December 10, 2013

dx.doi.org/10.1021/jp410229u | J. Phys. Chem. B 2013, 117, 16522−16529

gaps. Multiple modeling paradigms are needed,[11] because processes such as proton hopping, water clustering, and polymer fluctuations happen on different length and time scales, and we do not yet have a single scheme that can seamlessly bridge these disparate scales. A representative selection of previous computational work on Nafion includes quantum chemical calculations,[7,12,13] studies using empirical valence bond models,[14−19] ab initio molecular dynamics (AIMD) simulations,[20−24] quantum hopping MD[25] and classical MD simulations,[26−36] and mesoscale modeling studies.[37−40]

Previous work using density functional theory (DFT) calculations[12] has shown that proton transfer from the acid group in Nafion to H_2O requires a λ value of three or higher. Classical MD simulations[25] show that the H_2O molecules form isolated clusters around SO_3^- groups for $\lambda < 5$, and these clusters start to connect and form a percolation network with λ increasing above 5. The limitations of the classical description of the proton as H_3O^+ were illustrated by Petersen et al's multistate empirical valence bond simulations[16] of Nafion for two λ values. This group subsequently decomposed proton transport into proton hopping and vehicular transport components,[19] and found them to be of similar magnitude but anticorrelated resulting in overall proton diffusion being smaller than the individual components. A more recent simulation[17] of proton solvation and transport in Nafion using a self-consistent iterative multistate empirical valence bond method has revealed the influence of sulfonate groups on the proton hydration structure. Proton hopping and vehicular proton transport were again found to be strongly anticorrelated. The overall proton diffusion coefficient was in good agreement with experimental observations[41] for λ values of 6, 10 and 15, although the vehicular diffusion coefficient was higher than the proton diffusion coefficient from experiment by a factor of about 3.

One of the most fundamental issues in proton transport is the complex dynamics of the proton as it takes advantage of the surrounding water molecules to hop across hydrogen bonded clusters rather than to just follow the vehicular diffusion of the water molecule to which it is attached at a given instant. For complex molecular environments, such as those encountered in PEMs, theoretical methods that aim to describe proton transport accurately at the molecular level need to capture this dynamical distortion. This capability is inherent to ab initio method, and recent studies[20−24] have employed AIMD simulations of multiple protons in hydrated Nafion to place proton dynamics on a firm ab initio footing. Choe et al.[21] used AIMD simulations of proton transport in a simple Nafion system containing two monomers for about 20 ps. Two λ values, 4.25 and 12.75, were studied. These authors found the barrier for the transition from a contact ion pair (CIP) with the sulfonate group to a solvent-separated ion pair to be quite high for the lower λ value. However, the calculated proton diffusion coefficients were much higher than experimental values.[41] Habenicht et al.[22] used AIMD simulations to examine proton transfer in single walled carbon nanotubes with tethered CF_2SO_3H groups for λ values from 1 to 3 (nearly dry membrane model). At these low hydration levels, the dissociated proton was found to exist mainly as a H_3O^+ ion. Ilhan and Spohr[24] studied H_2O molecules in a simulated Nafion pore using AIMD. The protons were found to dissociate and form CIPs at $\lambda = 3$. Increasing the hydration level to 4.5 increased the population of $H_5O_2^+$−like configurations. However, one of the dimensions of the simulation cell was very small (5.4 Å), and this led to artifacts from S atoms interacting with their own periodic image. In the present work, we have performed AIMD simulation of proton hopping at three different hydration levels, λ values of 3, 9, and 15, in a large Nafion simulation cell ($\sim 20 \times 24 \times 27$ Å) previously equilibrated using classical molecular dynamics (MD) simulations. Our results provide fundamental molecular level insights into proton hopping in a model PEM.

II. COMPUTATIONAL DETAILS

We equilibrated models of hydrated Nafion using classical MD simulations with the DL_POLY_3 code[42] for λ values of 3, 9, and 15 at 300 K. These λ values were chosen to represent dry, hydrated, and saturated Nafion membrane, respectively. All the sulfonate groups were ionized, which is a reasonable assumption for the hydration levels examined based on prior work.[12] H_3O^+ served as the counterion. We used the DREIDING force field for Nafion and H_3O^+,[27,43] and F3C force field for H_2O molecules.[44] We have discussed the equilibration scheme in detail previously.[31,32] The chemical structure of a single chain of Nafion with 10 SO_3^- groups, as used in the present work, is shown in Figure I of the Supporting Information section. The SO_3^--terminated side chains are separated by seven nonpolar ($-CF_2-CF_2-$) monomers that constitute a hydrophobic backbone. The Nafion chain formed by linking 10 sets of alternating polar and nonpolar monomeric units and capping the ends of the chain with F had 682 atoms. In addition to the 10 H_3O^+ ions, we added a number of water molecules, ranging from 20 to 140, in accordance with the λ value. After energy minimization and annealing, our equilibrated systems had densities of 1.61, 1.88, and 1.67 g/cm^3 for λ of 3, 9 and 15, respectively. The corresponding experimental values[45] are in the range from 1.7 to 1.96 g/cm^3.

We utilized the equilibrated Nafion systems as the starting configurations for Born−Oppenheimer molecular dynamics simulations at 300 K using the CP2K code[46] with the PBE functional.[47] The simulations were performed with the constant NVT ensemble (number of atoms, volume and temperature). We used the GTH pseudopotentials[48] and the DZVP-MOLOPT basis set[49] with a density cutoff of 280 Ry for water and SZV-MOLOPT basis set for Nafion,[49] periodic boundary conditions, and time step of 0.5 fs. The simulation cell dimensions were about $19 \times 24 \times 27$ Å, $19 \times 23 \times 27$ Å, and $22 \times 23 \times 28$ Å with 782, 962, and 1142 atoms, respectively for $\lambda = 3$, 9, and 15 respectively. The simulations for $\lambda = 3$, 9, and 15 were run for 130, 75, and 75 ps, respectively, with the final 35−60 ps used for data analysis. We calculated radial distribution functions, water network percolation probability,[25,50] proton population distribution, and potentials of mean force. For the purpose of population analysis, we assigned the proton to the nearest oxygen if the O−H distance was within 1.3 Å. A proton was considered to have transferred to the sulfonate group, if the closest oxygen belonged to a sulfonate and the O−H distance was within 1.3 Å. We set the O−O cutoff distance to 2.6 Å to identify CIPs and cations such as $H_5O_2^+$, $H_7O_3^+$, and $H_9O_4^+$. The structure of these cations can be seen in Figures II, III, and IV, respectively, of the Supporting Information. The current simulations involve bigger system sizes, longer simulation times, and wider range of λ values than prior AIMD work on Nafion.[20−24]

dx.doi.org/10.1021/jp410229u | J. Phys. Chem. B 2013, 117, 16522−16529

III. RESULTS AND DISCUSSION

The water network in Nafion obtained from a configuration for λ = 15 is shown in perspective projection in Figure 1. Only the

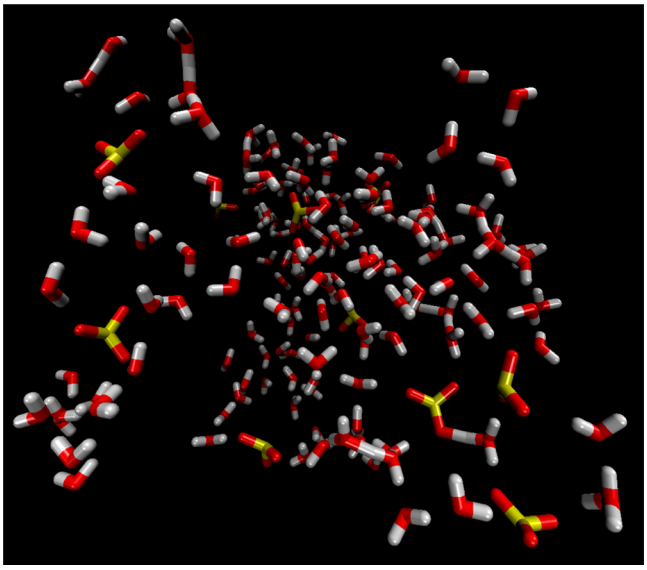

Figure 1. Perspective projection from a hydrated Nafion configuration for λ = 15. O, H, and S are shown in red, white, and yellow, respectively. The CF_2 groups are not shown to reduce clutter.

sulfonate groups, hydrated protons, and water molecules are shown for the sake of clarity. One can see $H_5O_2^+$ and $H_7O_3^+$ cations in the upper left and a CIP in the lower right. It is interesting to note that the SO_3^- group can bind the H_3O^+ cation even at a high level of hydration. The water molecules form wires between the sulfonate groups. The picture presented here is a snapshot from a certain time step and one must bear in mind that there are dynamic changes in the environment of the protons during the simulation. In our analysis, we first assign a proton to the nearest O and then determine its nature based on the presence of water oxygens and sulfonate oxygens within 2.6 Å of the O associated with the proton. We analyzed the data at each time step (0.5 fs interval) and averaged our results over nearly 100 000 such snapshots for each λ.

The probability of finding the proton in different configurations is plotted in Figure 2 for three hydration levels. For λ = 3, the proton resides on the sulfonate group about 6.6% of the time. We use the notation SO_3H to represent this occurrence. Table 1 lists the probabilities of occurrence of different cations and the percolation probability. It is interesting to note that there is a small probability (0.05%) that the proton will transfer to the sulfonate even for λ = 15. The H_3O^+ notation does not imply free H_3O^+ ions, because it includes CIPs, i.e., H_3O^+ bound to SO_3^-. The probability of finding the proton locked up as SO_3H or in a CIP is about 0.81 for λ = 3, and this value drops drastically to about 0.17 for λ =15.

In an effort to understand the CIP in hydrated Nafion, we have plotted the proton population distribution as a function of the reaction coordinate between the sulfonate oxygen and hydronium oxygen ($r_{OsH} - r_{OhH}$) in Figure 3. Negative values of the abscissa represent the sulfonate end and positive values the hydronium end of the ion pair. For λ = 3, some of the proton population is found toward the sulfonate end, which represents proton transfer to the sulfonate group. For λ = 9 and

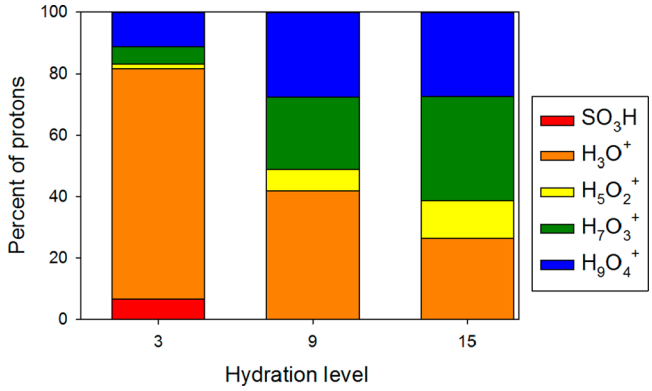

Figure 2. Percent of time spent by protons in different molecular arrangements in Nafion averaged over the AIMD trajectory: bound to SO_3^- (red), H_3O^+ including contact ion pair (orange), $H_5O_2^+$ (yellow), $H_7O_3^+$ (green) and $H_9O_4^+$ (blue) for λ = 3, 9, and 15. The cations were identified based on cutoff distances for O−H and O−O of 1.3 and 2.6 Å, respectively.

15, the proton population shifts almost entirely to the hydronium end. The peak height decreases with increasing λ, which indicates that the probability of forming a CIP or transferring the proton to the sulfonate group, decreases progressively.

Corresponding to the above change in proton population, Table 1 shows that the availability of protons for hopping, represented by the probability of finding a proton as $H_5O_2^+$ or $H_7O_3^+$ or $H_9O_4^+$, increases from 0.185 to 0.736 with λ increasing from 3 to 15. In addition to the proton, most of the water molecules are bound to the sulfonate group (defined in terms of the sulfur-water oxygen distance being less than 4.3 Å) at low hydration. The probability of H_2O being bound decreases from 0.743 to 0.243 as λ increases from 3 to 15. The decrease in bound H_2O and the increase in the overall number of H_2O molecules (N) are conducive to water network percolation. The percolation probability, defined here as the probability that a given water molecule will belong to a cluster of size greater than $N/2$, increases from 0 at λ = 3 to 0.99 at λ = 15. Increasing the hydration level sets the proton free from the sulfonate group, reduces the binding of water molecules to SO_3^- thereby increasing the likelihood of a hydrated environment ($H_5O_2^+$, $H_7O_3^+$, or $H_9O_4^+$) for the proton, and creates a percolating cluster across which the proton is free to hop. From Figures II, III, and IV of the Supporting Information, it is clear that the cations identified as $H_7O_3^+$ and $H_9O_4^+$ are most likely to be Zundel ($H_5O_2^+$) cations with one or two water molecules in close proximity (O−O distance less than 2.6 Å). In poorly hydrated Nafion, the proton exists mostly as a free or bound H_3O^+, and it may also reside with the acid group of the pendant. In well-hydrated Nafion, the proton is mostly found as a Zundel cation with proximate water molecules that can act as proton acceptors.

We have calculated the potential of mean force (PMF) based on the radial distribution of the proton relative to the sulfonate oxygen and the PMF is shown in Figure 4. For λ = 3, the energy barrier for the proton to transfer from a CIP to a solvent separated ion pair is 2.3 kcal/mol. At the intermediate λ of 9, this barrier decreases to 2.1 kcal/mol. This barrier decreases considerably to 0.8 kcal/mol for λ = 15. The larger barrier for λ = 3 provides an explanation for the high probability of forming CIPs at the low hydration level. Figure 5 is a plot of the energy

dx.doi.org/10.1021/jp410229u | J. Phys. Chem. B 2013, 117, 16522−16529

Table 1. Probabilities of Percolation and Occurrence of Cations in Hydrated Nafion

hydration level (λ)	probability of SO_3H	probability of SO_3H or contact ion pair	probability of $H_5O_2^+$ or $H_7O_3^+$ or $H_9O_4^+$	probability of bound H_2O	percolation probability
3	0.066	0.812	0.185	0.743	0.00
9	0.001	0.289	0.581	0.499	0.91
15	0.0005	0.173	0.736	0.243	0.99

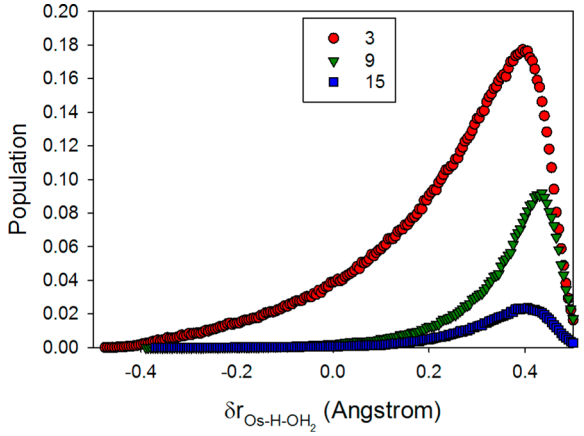

Figure 3. Proton population as a function of the contact ion pair reaction coordinate for three hydration levels indicated by the legend. The reaction coordinate is the difference between the distances to the H from the sulfonate oxygen and water oxygen. The abscissa goes from the sulfonate end on the left to the hydronium end on the right.

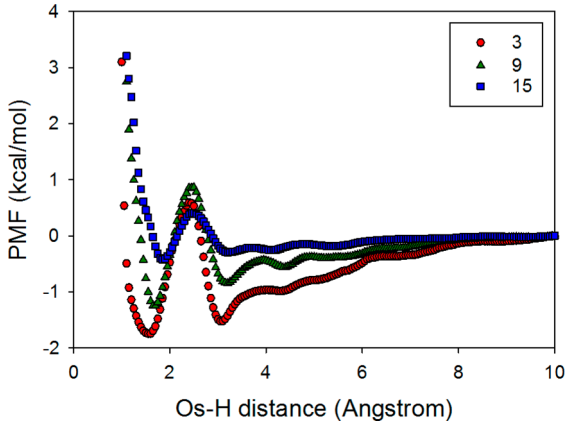

Figure 4. Potential of mean force as a function of distance between sulfonate oxygen and hydrogen for three different hydration levels indicated by the legend.

barrier for proton transfer as a function of λ, and includes the results from the AIMD simulations of Choe et al.[21] The two sets of results are consistent and show that the proton transfer barrier decreases significantly between λ =9 and λ=15. The water network percolation probability is similar at these two hydration levels, but the probability of forming $H_5O_2^+$, $H_7O_3^+$, or $H_9O_4^+$ is quite different (0.58 vs 0.73). Recent work[51] has shown that these cations play an important role in proton hopping under confinement. Cao et al.[51] simulated proton hopping along water networks in carbon nanotubes and found that proton transfer in such confined molecular environments occurs by a Zundel–Zundel mechanism through a $H_7O_3^+$ cation rather than the Eigen ($H_9O_4^+$)–Zundel–Eigen mechanism proposed to explain proton transport in bulk water. The carbon nanotubes studied by Cao et al.[51] feature confinement.

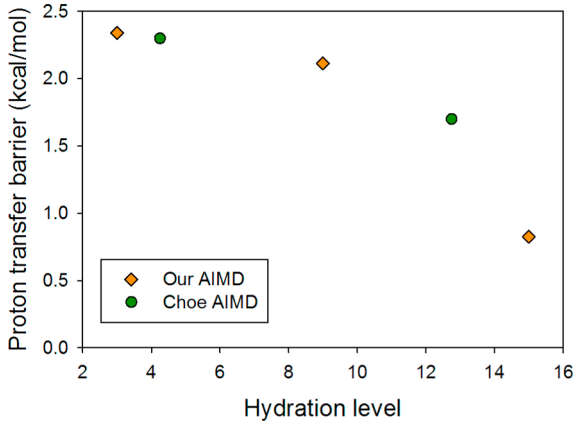

Figure 5. Energy barrier for proton transfer from a contact ion pair to a solvent-separated ion pair. The results from the AIMD simulations of Choe et al.[21] (circles) are included for comparison.

The present model system combines confinement with a complex chemical environment. The proton transfer mechanism in Nafion appears to be similar to that reported in the confined environment of carbon nanotubes and unlike the mechanism in bulk water. From Figure 1, it is easy to visualize how small changes in the water network brought by H_2O diffusion can bring about dynamic changes in the structure of the hydrated proton.

The barrier for proton transfer between two water molecules can be determined from the free energy profile as a function of the reaction coordinate between two water molecules plotted in Figure 6. The reaction coordinate[52] is the difference between the two O–H distances. The plots for the three hydration levels are staggered for the sake of clarity. The energy barrier was found to lie between 0.7 and 0.8 kcal/mol for the hydration

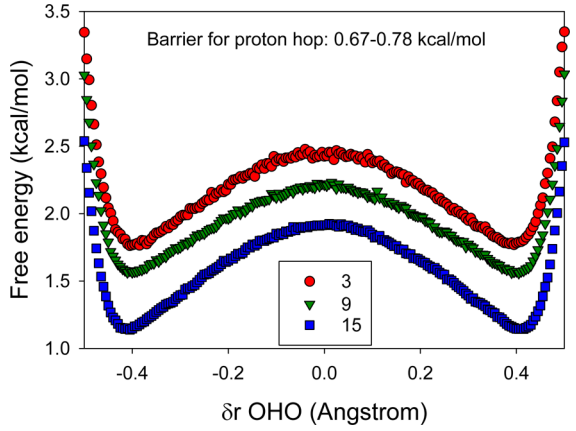

Figure 6. Proton transfer barrier for three hydration levels in Nafion. The abscissa is the reaction coordinate ($r_{O1H} - r_{O2H}$), where O1 and O2 are the oxygens of the two water molecules involved in proton transfer. The plots for the different hydration levels have been displaced with respect to each other for clarity.

dx.doi.org/10.1021/jp410229u | J. Phys. Chem. B 2013, 117, 16522–16529

levels examined, and no clear trend could be discerned with respect to hydration level. This is comparable to the barrier of 0.6 kcal/mol obtained by a previous study[52] for protonic defect in bulk water. Regardless of λ, the barrier is quite small and nearly the same. The main obstacle to proton hopping in Nafion appears to be the binding of the hydrated proton by the sulfonate group.

We have classified proton transfer events into shuttles (proton going back and forth between two oxygens O1 and O2) and hops (proton transferring to a third oxygen O3 following shuttles between O1 and O2). Choe et al.[21] refer to shuttles and hops as nonconstructive and constructive proton transfer, respectively. They found that nonconstructive transfer (shuttle) occurs more readily at λ = 4.25 compared to the case of λ = 12.75. We find that proton shuttling is dominant at all hydration levels, which is consistent with the similar low proton transfer barriers shown in Figure 6. Most of the shuttling at λ = 3 occurs in the CIP formed with the sulfonate oxygen. We calculated the ratio of shuttles per hop overall and excluding the CIP. The ratios are shown in Figure V of the Supporting Information. If we include the shuttling in the CIP, the ratio of shuttles to hops decreases from 22.6 for λ = 3 to 9.5 for λ = 15. However, if we exclude the CIP shuttles, the change in this ratio is much smaller—from 12.9 for λ = 3 to 9.5 for λ = 15. The proton is unlikely to transfer back to the sulfonate group for λ = 9 and 15, the probability of forming a CIP is reduced, and the probability of forming a percolating water cluster is high at these hydration levels (see Table 1). Figure VI of the Supporting Information shows the time per hop obtained by dividing the production time by the number of hops per proton. As λ increases from 3 to 15, the time per hop decreases from 1.9 to 0.5 ps. The formation of CIP and the break in the hydrogen bonded network at low hydration levels are key factors in increasing the time per hop at the low hydration level.

In addition to the time between proton hops, the location of hopping events in the water-filled pores of Nafion is of considerable interest. We have calculated the distribution of the distance of the oxygens of proton donors and proton acceptors from the nearest sulfur atom. The donor and acceptor distance distributions were nearly similar. Figure 7 is a plot of the donor distances for proton hops (constructive transfers) for the three λ values studied. In nearly dry Nafion (λ = 3), most of the hops involve the contact ion pair and the distribution has a strong peak around 3.6 Å. Hopping did not occur at a O−S distance greater than 5.6 Å. At intermediate hydration (λ = 9), the peak of the distribution shifts to 3.8 Å and the maximum O−S distance observed was 7.5 Å. Finally, in well hydrated Nafion (λ = 15), the proton donor distance distribution shows a prominent peak at 5.5 Å, but interestingly a strong second peak appears at about 7.7 Å. In fact, proton hopping events occur as far as 9.9 Å away from the nearest S. This distance is consistent with small-angle X-ray scattering results[10] that yield an average water cluster diameter in hydrated Nafion of 24 Å. At λ = 15, the hydrated proton is able to reach the center of the water channel, which facilitates good proton conductivity. Since the proton acceptor distances also show a similar distribution, an effect of increasing the hydration level is to shift the proton hopping events away from the sulfonate groups.

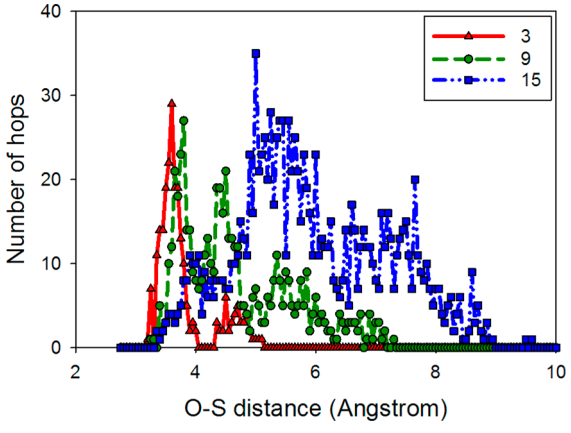

Figure 7. Distribution of the distance between the oxygen of the proton donor and the nearest sulfur in Nafion.

The average distance from the nearest sulfur atom for H_2O, H_3O^+ (here H_3O^+ represents all the hydrated protons in the system), proton donor, and proton acceptor is plotted in Figure VII of the Supporting Information. All of these species move away from the sulfonate group as λ increases. At the lowest hydration level (λ = 3), H_3O^+ is closer to the SO_3^- than H_2O, because CIPs are predominant. The average proton donor is farther (by 0.02 to 0.2 Å) than the average proton acceptor relative to the nearest S atom. Thus, the average proton jump is slightly toward the sulfonate group.

The changes in the distribution of the sulfonate groups that go along with the above changes in water and hydrated proton distribution can be inferred from the S−S coordination number plotted as a function of radial distance in Figure 8. The

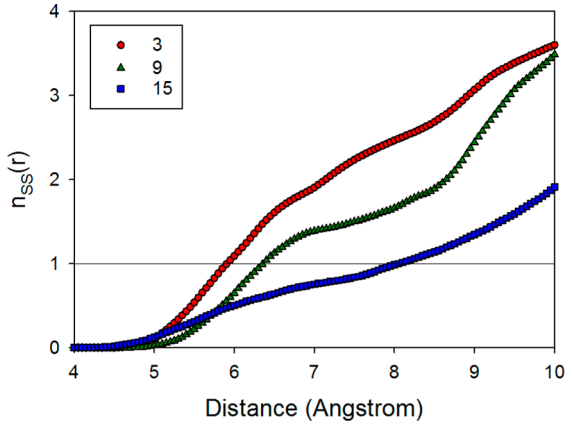

Figure 8. Sulfur−sulfur coordination number as a function of radial distance for hydration levels indicated by the legend.

sulfonate groups are clustered close together for λ = 3, and they move apart with increasing hydration level. The radial distance from a given S within which one can find another S, indicated by the horizontal line at coordination number of 1, is 5.9 Å for λ = 3, 6.35 Å for λ = 9, and 8.05 Å for λ = 15. It is known from previous classical MD simulations[53] that the pore diameter of PEMs increases with increasing hydration level. Figure 9 shows the index of the nearest S atom from a given proton for λ = 15. Even though the sulfonate groups are well separated at this hydration level, the proton visits six different sulfonate groups in about 60 ps. This is an indication of the mobility of the proton at the high hydration level.

Further proof of the mobility of the proton can be obtained by examining the identity of the water oxygen associated with the proton as a function of simulation time. We have plotted this index for one proton chosen to represent λ = 3 and another

dx.doi.org/10.1021/jp410229u | J. Phys. Chem. B 2013, 117, 16522−16529

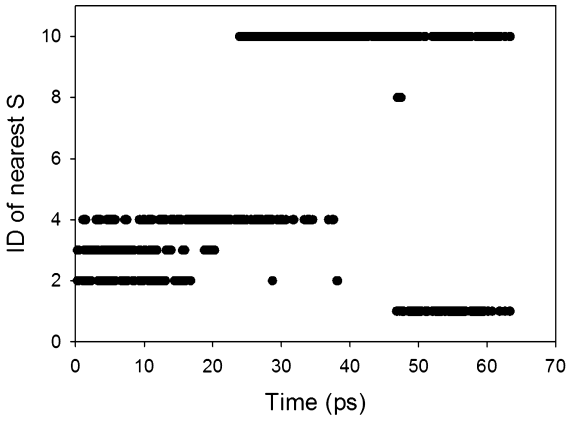

Figure 9. The index of the nearest S atom for a given hydrated proton for $\lambda = 15$.

proton for $\lambda = 15$ in Figure 10. For $\lambda = 3$, the proton is predominantly associated with one water molecule and hops to

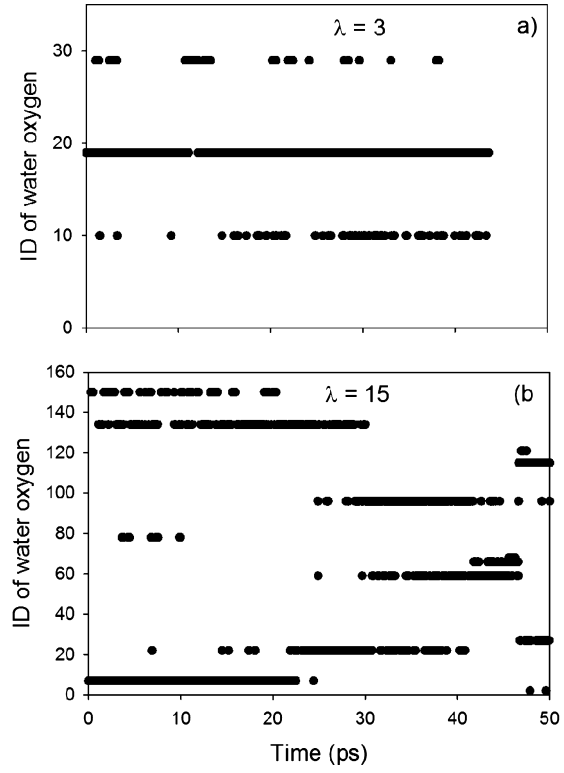

Figure 10. The index of the oxygen associated with a proton in Nafion for (a) $\lambda = 3$ and (b) $\lambda = 15$. The proton hops between more water molecules at the higher λ.

two other water molecules. In contrast, the proton visits multiple water molecules for $\lambda = 15$. In well-hydrated Nafion, the proton hops across many water molecules, visits several sulfonate groups, but stays on the average about 5.6 Å from the S atom (S−O distance).

Figure 11 shows the overall proton diffusion coefficient for $\lambda = 15$ from the present work along with the vehicular hydronium diffusion coefficient from classical molecular dynamics simulations, and experimental proton diffusion coefficients from the work of Zawodzinski et al.[41] We calculated the diffusion coefficient from the mean square displacement (MSD) of the

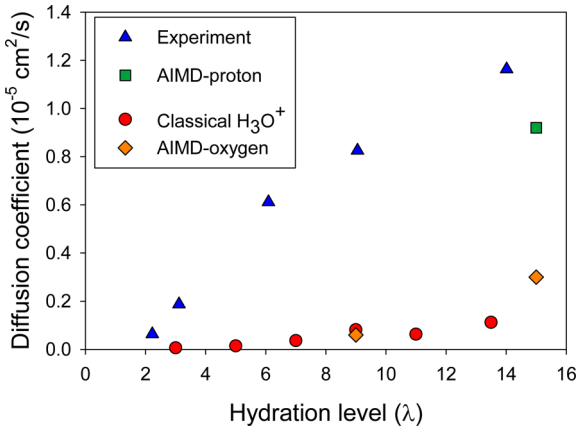

Figure 11. Overall proton diffusion coefficient from the present AIMD simulation for $\lambda = 15$ (square) compared to experimental[41] proton diffusion data (triangles), vehicular H_3O^+ diffusion coefficient from classical MD simulations (circles),[32] and water/hydronium oxygen diffusion coefficient from AIMD simulation (diamonds).

oxygen associated with the proton using the Einstein relation shown in eq 1

$$D = \lim_{t\to\infty} \frac{1}{6t}\langle|\vec{r}(t) - \vec{r}(0)|^2\rangle \quad (1)$$

where the numerator is the MSD and t is time. We fit the MSD versus t relationship using linear least-squares regression. Since the trajectories are short (tens of ps) as a result of the computational intensity of the calculation, the coefficient of determination (R^2) was small for $\lambda = 3$ ($R^2 = 0.68$) and $\lambda = 9$ ($R^2 = 0.21$). We obtained a reliable fit ($R^2 = 0.91$) for $\lambda = 15$, and the calculated diffusion coefficient was 0.9×10^{-5} cm^2/s. This value is in good agreement with experimental data for proton diffusion.[41] The MSD for $\lambda = 15$ is plotted against time in Figure VIII of the Supporting Information.

We have also calculated the MSD for all water oxygens (this includes water molecules and hydronium ions) from the AIMD trajectories. The oxygen MSD for $\lambda = 3$ showed no time dependence, which indicates a lack of water diffusion at low hydration. For $\lambda = 9$ and 15, as shown in Figure IX of the Supporting Information, the oxygen MSD increased linearly with time. The diffusion coefficients obtained by linear least-squares regression are 0.06×10^{-5} cm^2/s for $\lambda = 9$ ($R^2 = 0.81$) and 0.3×10^{-5} cm^2/s for $\lambda = 15$ ($R^2 = 0.96$). These values, represented in Figure 11 as diamonds, are consistent with the H_3O^+ diffusion coefficients obtained from our previous classical MD simulations.[32] This consistency serves to validate the previous classical MD simulations of vehicular proton transport.

We found that the water oxygen diffusion coefficient for $\lambda = 15$ is the same as the water oxygen diffusion coefficient that we obtained in an AIMD simulation with the NVE ensemble of a single proton and 64 water molecules at 300 K (0.3×10^{-5} cm^2/s) with the same basis set and pseudopotentials used for water in hydrated Nafion. This agreement indicates that the water molecules at $\lambda = 15$ are in a bulk-like environment. At $\lambda = 9$, the water diffusion is slower than in bulk water due to binding by the sulfonate group. At $\lambda = 3$, the diffusion of water molecules is extremely slow. Our simulations do not show evidence of the highly enhanced vehicular proton diffusion reported in a previous work.[17] Our results viewed in the light of experimental findings and previous classical MD simulations of vehicular hydronium transport show that proton conductivity

dx.doi.org/10.1021/jp410229u | J. Phys. Chem. B 2013, 117, 16522−16529

in fuel cell membranes is dominated by proton hopping at all hydration levels. The present study has presented a molecular-level picture of proton and water dynamics as a function of hydration in the complex chemical environment of a model fuel cell membrane.

IV. CONCLUSIONS

We have performed ab initio molecular dynamics simulations of proton hopping in the Nafion polymer membrane for hydration levels (λ) of 3, 9, and 15 H_2O/SO_3^-. The hydrated proton is mainly bound to the sulfonate group in the form of a contact ion pair in the nearly dry membrane ($\lambda = 3$). The proton can also transfer to the sulfonate group at this low hydration level. As λ increases, the barrier for proton transfer from contact ion pair to solvent separated ion pair decreases, the water molecules form a percolating cluster, and the proton is able to hop through the water network visiting multiple sulfonate groups. In the confined environment of the membrane, the protonic defect exists as $H_5O_2^+$, $H_7O_3^+$, and $H_9O_4^+$ cations for λ values of 9 and 15, in agreement with experimental observations on protons confined to nanotubes. Our proton diffusion coefficient 0.9×10^{-5} cm^2/s for $\lambda = 15$ agrees with experimental trends and points to the dominance of hopping over vehicular proton transport in hydrated Nafion.

■ ASSOCIATED CONTENT

Supporting Information

Chemical structures of a single chain of Nafion, $H_5O_2^+$, $H_7O_3^+$, and $H_9O_4^+$; the ratio of proton shuttles to proton hops as a function of hydration level; time elapsed between proton hops in hydrated Nafion; distance from the nearest S in hydrated Nafion to the oxygen of H_2O or H_3O^+; plot of proton mean square displacement as a function of time for $\lambda = 15$ in Nafion; and plot of oxygen (water and hydronium oxygen) mean square displacement as a function of time for $\lambda = 9$ and $\lambda = 15$ in Nafion. This material is available free of charge via the Internet at http://pubs.acs.org.

■ AUTHOR INFORMATION

Corresponding Author

*E-mail: ram.devanathan@pnnl.gov; Phone: 1-509-371-6487.

Notes

The authors declare no competing financial interest.

†Deceased 11 March 2012.

■ ACKNOWLEDGMENTS

This work was supported by the U.S. Department of Energy (DOE), Office of Basic Energy Sciences, Division of Chemical Sciences, Geosciences & Biosciences. This research used resources of the National Energy Research Scientific Computing Center, which is supported by the Office of Science of the U.S. Department of Energy under Contract No. DE-AC02-05CH11231. M.D.B. is grateful for the support of the Linus Pauling Distinguished Postdoctoral Fellowship Program at Pacific Northwest National Laboratory (PNNL). PNNL is a multiprogram national laboratory operated for DOE by Battelle.

■ REFERENCES

(1) Voth, G. A. Computer Simulation of proton solvation and transport in aqueous and biomolecular systems. *Acc. Chem. Res.* **2006**, *39*, 143−150.

(2) Cukierman, S. Et tu, Grotthuss! and other unfinished stories. *Biochim. Biophys.Acta - Bioenergetics* **2006**, *1757*, 876−885.

(3) Gust, D.; Moore, T. A.; Moore, A. L. Mimicking photosynthetic solar energy transduction. *Acc. Chem. Res.* **2000**, *34*, 40−48.

(4) Yang, C.; Costamagna, P.; Srinivasan, S.; Benziger, J.; Bocarsly, A. B. Approaches and technical challenges to high temperature operation of proton exchange membrane fuel cells. *J. Power Sources* **2001**, *103*, 1−9.

(5) Devanathan, R. Recent developments in proton exchange membranes for fuel cells. *Energy Environ. Sci.* **2008**, *1*, 101−119.

(6) Mauritz, K. A.; Moore, R. B. State of understanding of Nafion. *Chem. Rev.* **2004**, *104*, 4535−4585.

(7) Elliott, J. A.; Paddison, S. J. Modelling of morphology and proton transport in PFSA membranes. *Phys. Chem. Chem. Phys.* **2007**, *9*, 2602−2618.

(8) Kreuer, K. D.; Paddison, S. J.; Spohr, E.; Schuster, M. Transport in proton conductors for fuel-cell applications: Simulations, elementary reactions, and phenomenology. *Chem. Rev.* **2004**, *104*, 4637−4678.

(9) Hsu, W. Y.; Gierke, T. D. Elastic theory for ionic clustering in perfluorinated ionomers. *Macromolecules* **1982**, *15*, 101−105.

(10) Schmidt-Rohr, K.; Chen, Q. Parallel cylindrical water nanochannels in Nafion fuel-cell membranes. *Nat. Mater.* **2008**, *7*, 75−83.

(11) Goddard, W.; Merinov, B.; Van Duin, A.; Jacob, T.; Blanco, M.; Molinero, V.; Jang, S. S.; Jang, Y. H. Multi-paradigm multi-scale simulations for fuel cell catalysts and membranes. *Mol. Simulat.* **2006**, *32*, 251−268.

(12) Paddison, S. J. The modeling of molecular structure and ion transport in sulfonic acid based ionomer membranes. *J. New Mater. Electrochem. Syst.* **2001**, *4*, 197−207.

(13) Paddison, S. J.; Elliott, J. A. Molecular modeling of the short-side-chain perfluorosulfonic acid membrane. *J. Phys. Chem. A* **2005**, *109*, 7583−7593.

(14) Spohr, E.; Commer, P.; Kornyshev, A. A. Enhancing proton mobility in polymer electrolyte membranes: Lessons from molecular dynamics simulations. *J. Phys. Chem. B* **2002**, *106*, 10560−10569.

(15) Kornyshev, A. A.; Kuznetsov, A. M.; Spohr, E.; Ulstrup, J. Kinetics of proton transport in water. *J. Phys. Chem. B* **2003**, *107*, 3351−3366.

(16) Petersen, M. K.; Wang, F.; Blake, N. P.; Metiu, H.; Voth, G. A. Excess proton solvation and delocalization in a hydrophilic pocket of the proton conducting polymer membrane Nafion. *J. Phys. Chem. B* **2005**, *109*, 3727−3730.

(17) Feng, S.; Voth, G. A. Proton solvation and transport in hydrated Nafion. *J. Phys. Chem. B* **2011**, *115*, 5903−5912.

(18) Feng, S. L.; Savage, J.; Voth, G. A. Effects of polymer morphology on proton solvation and transport in proton-exchange membranes. *J. Phys. Chem. C* **2012**, *116*, 19104−19116.

(19) Petersen, M. K.; Voth, G. A. Characterization of the solvation and transport of the hydrated proton in the perfluorosulfonic acid membrane Nafion. *J. Phys. Chem. B* **2006**, *110*, 18594−18600.

(20) Roudgar, A.; Narasimachary, S. P.; Eikerling, M. Ab initio study of surface-mediated proton transfer in polymer electrolyte membranes. *Chem. Phys. Lett.* **2008**, *457*, 337−341.

(21) Choe, Y.-K.; Tsuchida, E.; Ikeshoji, T.; Yamakawa, S.; Hyodo, S.-A. Nature of proton dynamics in a polymer electrolyte membrane, Nafion: a first-principles molecular dynamics study. *Phys. Chem. Chem. Phys.* **2009**, *11*, 3892−3899.

(22) Habenicht, B. F.; Paddison, S. J.; Tuckerman, M. E. The effects of the hydrophobic environment on proton mobility in perfluorosulfonic acid systems: an ab initio molecular dynamics study. *J. Mater. Chem.* **2010**, *20*, 6342−6351.

(23) Ilhan, M. A.; Spohr, E. Ab initio molecular dynamics of proton networks in narrow polymer electrolyte pores. *J. Phys.: Condens. Matter* **2011**, *23*, 234104.

(24) Ilhan, M. A.; Spohr, E. Hydrogen bonding in narrow protonated polymer electrolyte pores. *J. Electroanal. Chem.* **2011**, *660*, 347−351.

(25) Devanathan, R.; Venkatnathan, A.; Rousseau, R.; Dupuis, M.; Frigato, T.; Gu, W.; Helms, V. Atomistic simulation of water

percolation and proton hopping in Nafion fuel cell membrane. *J. Phys. Chem. B* **2010**, *114*, 13681−13690.
(26) Vishnyakov, A.; Neimark, A. V. Molecular dynamics simulation of microstructure and molecular mobilities in swollen Nafion membranes. *J. Phys. Chem. B* **2001**, *105*, 9586−9594.
(27) Jang, S. S.; Molinero, V.; Cagin, T.; Goddard, W. A. Nanophase-segregation and transport in Nafion 117 from molecular dynamics simulations: Effect of monomeric sequence. *J. Phys. Chem. B* **2004**, *108*, 3149−3157.
(28) Urata, S.; Irisawa, J.; Takada, A.; Shinoda, W.; Tsuzuki, S.; Mikami, M. Molecular dynamics simulation of swollen membrane of perfluorinated ionomer. *J. Phys. Chem. B* **2005**, *109*, 4269−4278.
(29) Cui, S. T.; Liu, J. W.; Selvan, M. E.; Keffer, D. J.; Edwards, B. J.; Steele, W. V. A molecular dynamics study of a Nafion polyelectrolyte membrane and the aqueous phase structure for proton transport. *J. Phys. Chem. B* **2007**, *111*, 2208−2218.
(30) Venkatnathan, A.; Devanathan, R.; Dupuis, M. Atomistic simulations of hydrated Nafion and temperature effects on hydronium ion mobility. *J. Phys. Chem. B* **2007**, *111*, 7234−7244.
(31) Devanathan, R.; Venkatnathan, A.; Dupuis, M. Atomistic simulation of Nafion membrane: I. Effect of hydration on membrane nanostructure. *J. Phys. Chem. B* **2007**, *111*, 8069−8079.
(32) Devanathan, R.; Venkatnathan, A.; Dupuis, M. Atomistic simulation of Nafion membrane. 2. Dynamics of water molecules and hydronium ions. *J. Phys. Chem. B* **2007**, *111*, 13006−13013.
(33) Liu, J.; Selvan, M. E.; Cui, S.; Edwards, B. J.; Keffer, D. J.; Steele, W. V. Molecular-level modeling of the structure and wetting of electrode/electrolyte interfaces in hydrogen fuel cells. *J. Phys. Chem. C* **2008**, *112*, 1985−1993.
(34) Selvan, M. E.; Keffer, D. J.; Cui, S.; Paddison, S. J. A reactive molecular dynamics algorithm for proton transport in aqueous systems. *J. Phys. Chem. C* **2010**, *114*, 11965−11976.
(35) Knox, C. K.; Voth, G. A. Probing selected morphological models of hydrated Nafion using large-scale molecular dynamics simulations. *J. Phys. Chem. B* **2010**, *114*, 3205−3218.
(36) Brandell, D.; Karo, J.; Liivat, A.; Thomas, J. O. Molecular dynamics studies of the Nafion®, Dow® and Aciplex® fuel-cell polymer membrane systems. *J. Mol. Model.* **2007**, *13*, 1039−1046.
(37) Wescott, J. T.; Qi, Y.; Subramanian, L.; Capehart, T. W. Mesoscale simulation of morphology in hydrated perfluorosulfonic acid membranes. *J. Chem. Phys.* **2006**, *124*, 134702.
(38) Wu, D.; Paddison, S. J.; Elliott, J. A. A comparative study of the hydrated morphologies of perfluorosulfonic acid fuel cell membranes with mesoscopic simulations. *Energy Environ. Sci.* **2008**, *1*, 284−293.
(39) Dorenbos, G.; Suga, Y. Simulation of equivalent weight dependence of Nafion morphologies and predicted trends regarding water diffusion. *J. Membr. Sci.* **2009**, *330*, 5−20.
(40) Jorn, R.; Voth, G. A. Mesoscale simulation of proton transport in proton exchange membranes. *J. Phys. Chem. C* **2012**, *116*, 10476−10489.
(41) Zawodzinski, T. A.; Davey, J.; Valerio, J.; Gottesfeld, S. The water-content dependence of electroosmotic drag in proton-conducting polymer electrolytes. *Electrochim. Acta* **1995**, *40*, 297−302.
(42) Todorov, I. T.; Smith, W.; Trachenko, K.; Dove, M. T. DL_POLY_3: new dimensions in molecular dynamics simulations via massive parallelism. *J. Mater. Chem.* **2006**, *16*, 1911−1918.
(43) Mayo, S. L.; Olafson, B. D.; Goddard, W. A. DREIDING - A generic force-field for molecular simulations. *J. Phys. Chem.* **1990**, *94*, 8897−8909.
(44) Levitt, M.; Hirshberg, M.; Sharon, R.; Laidig, K. E.; Daggett, V. Calibration and testing of a water model for simulation of the molecular dynamics of proteins and nucleic acids in solution. *J. Phys. Chem. B* **1997**, *101*, 5051−5061.
(45) Morris, D. R.; Sun, X. D. Water-sorption and transport-properties of Nafion-117-H. *J. Appl. Polym. Sci.* **1993**, *50*, 1445−1452.
(46) VandeVondele, J.; Krack, M.; Mohamed, F.; Parrinello, M.; Chassaing, T.; Hutter, J. Quickstep: Fast and accurate density functional calculations using a mixed Gaussian and plane waves approach. *Comput. Phys. Commun.* **2005**, *167*, 103−128.
(47) Perdew, J. P.; Burke, K.; Ernzerhof, M. Generalized gradient approximation made simple. *Phys. Rev. Lett.* **1996**, *77*, 3865−3868.
(48) Goedecker, S.; Teter, M.; Hutter, J. Separable dual-space Gaussian pseudopotentials. *Phys. Rev. B* **1996**, *54*, 1703−1710.
(49) VandeVondele, J.; Hutter, J. Gaussian basis sets for accurate calculations on molecular systems in gas and condensed phases. *J. Chem. Phys.* **2007**, *127*, 114105.
(50) Brovchenko, I.; Krukau, A.; Oleinikova, A.; Mazur, A. K. Ion dynamics and water percolation effects in DNA polymorphism. *J. Am. Chem. Soc.* **2008**, *130*, 121−131.
(51) Cao, Z.; Peng, Y.; Yan, T.; Li, S.; Li, A.; Voth, G. A. Mechanism of fast proton transport along one-dimensional water chains confined in carbon nanotubes. *J. Am. Chem. Soc.* **2010**, *132*, 11395−11397.
(52) Marx, D.; Tuckerman, M. E.; Parrinello, M. Solvated excess protons in water: Quantum effects on the hydration structure. *J. Phys.: Condens. Matter* **2000**, *12*, A153.
(53) Devanathan, R.; Idupulapati, N.; Dupuis, M. Molecular modeling of the morphology and transport properties of two direct methanol fuel cell membranes: Phenylated sulfonated poly(ether ether ketone ketone) versus Nafion. *J. Mater. Res.* **2012**, *27*, 1927−1938.